

Adenosine Pathway-Based Prognostic Signature for Predicting Clinical Outcomes and Immune Microenvironment Characteristics in Epithelial Ovarian Cancer

 Akbar Ibrahimov,¹  Fidan Novruzova¹

¹Department of Oncology, Azerbaijan Medical University, Baku, Azerbaijan

ABSTRACT

Objective: This study aimed to develop and validate an adenosynergic prognostic signature for stratifying clinical outcomes and characterizing the tumor immune microenvironment in patients with EOC.

Materials and Methods: A retrospective bioinformatics analysis, complemented by experimental validation, was conducted. Adenosine signaling activity was quantified using ssGSEA, and key adenosynergic modules were identified using WGCNA. Prognostically significant adenosine-related genes (ARGs) were selected through LASSO Cox regression to construct a composite signature, which was then validated across multiple datasets. Functional enrichment analysis, immune infiltration estimation, and somatic alteration mapping were performed. *In vitro* validation in SK-OV-3 and A2780 cell lines included quantitative PCR, metabolic viability assays, scratch assays, and chamber-based invasion assessments.

Results: The blue module showed the strongest correlation with adenosine pathway activity. Nine independent prognostic ARGs were identified: 5 risk-associated genes (PIK3CG, VSIG4, MATK, PIEZO1, and RARRES1) and 4 protective genes (SELL, S1PR4, IL18BP, and CD40LG). The signature demonstrated robust time-dependent predictive accuracy for overall survival, with AUCs ranging from 0.62 at 1 year to 0.71 at 5 years (95% CI: 0.58–0.75 for 1 year, 0.63–0.71 for 3 years, and 0.67–0.75 for 5 years). High-risk patients exhibited significantly worse survival and inversely correlated CD8⁺ T-cell and macrophage infiltration ($p < 0.001$), suggesting impaired antitumor immunity. Somatic mutation analysis revealed co-occurrence patterns such as FAT3-MGA and MUC16-CSMD3 in high-risk cases. Experimental validation confirmed elevated ARG expression in cancer cells, and VSIG4 silencing significantly inhibited proliferation, migration, and invasion.

Conclusion: This study establishes a novel prognostic signature for stratifying OC outcomes. The model quantifies immunosuppressive microenvironmental features and identifies clinically actionable targets, particularly VSIG4, to guide treatment in EOC.

Keywords: Adenosine signaling, immune microenvironment, ovarian cancer, precision medicine, prognostic signature, VSIG4.



Cite this article as:

Ibrahimov A, Novruzova F. Adenosine Pathway-Based Prognostic Signature for Predicting Clinical Outcomes and Immune Microenvironment Characteristics in Epithelial Ovarian Cancer. J Clin Pract Res 2026;48(3):302–313.

Address for correspondence:

Akbar Ibrahimov.
Department of Oncology,
Azerbaijan Medical University,
Baku, Azerbaijan
Phone: +99 451 300 5252
E-mail:
dr.akbaribrahimov3@gmail.com

Submitted: 26.09.2025

Revised: 03.04.2026

Accepted: 10.06.2026

Available Online: 29.06.2026

Erciyes University Faculty of
Medicine Publications -
Available online at www.jcprres.com

Copyright © Author(s)
This work is licensed under
a Creative Commons
Attribution-NonCommercial
4.0 International License.



INTRODUCTION

Epithelial ovarian cancer (EOC) remains the most lethal gynecologic malignancy worldwide, accounting for ~5% of female cancer deaths and representing the leading cause of gynecological cancer mortality.¹ Despite therapeutic advances, the prognosis remains poor, with only 25% 5-year survival.² Characterized by asymptomatic progression and diffuse peritoneal dissemination, 70% of patients present with advanced-stage disease and peritoneal metastases at diagnosis.³ This clinical challenge is further exacerbated by profound molecular and phenotypic heterogeneity.⁴ High-grade serous ovarian carcinoma (HGSOC; 70% of cases) exhibits rapid progression, reaching advanced stages within ≤ 2 years.⁵ Although primary cytoreduction and platinum-based chemotherapy achieve initial responses, nearly three-quarters of patients with HGSOC develop chemoresistant recurrence, underscoring the critical need for novel biomarkers and targeted therapies.⁶

Cancer biology research now emphasizes the role of the tumor microenvironment (TME) in driving progression, metastasis, and chemoresistance.⁷ Specifically, in ovarian cancer, adenosine metabolism critically shapes an immunosuppressive TME landscape. The TME in ovarian carcinoma is particularly unique, generating malignant ascites that create favorable conditions for tumor cell survival, proliferation, and dissemination throughout the peritoneal cavity.⁸ This complex environment comprises immune, stromal, and fibroblastic cells, as well as biochemical factors such as adenosine-purinerigic metabolites, which significantly modulate TME immunosuppression in EOC. Additionally, it contains a diverse array of signaling molecules, growth factors, and metabolites that together affect tumor behavior and patient outcomes.⁹

Among the various metabolic and signaling pathways that regulate TME dynamics, adenosine signaling has emerged as a pivotal mechanism governing immune surveillance and tumor progression.¹⁰ Adenosine, an endogenous purine nucleoside, functions through four distinct adenosine receptors (A1, A2A, A2B, and A3) and affects cellular proliferation, differentiation, and apoptosis across various malignancies.¹¹ In cancer, adenosine accumulation in the TME represents a fundamental immunosuppressive mechanism that drives tumor immune escape via adenosine-induced cells and promotes disease progression.¹² The significance of the adenosine pathway in ovarian cancer has been increasingly recognized through recent research demonstrating its multifaceted roles in tumor biology.¹³ Through A2aR/A2bR engagement, adenosine drives TAM reprogramming into immunosuppressive and proangiogenic states.¹⁴ Critically, CD39- and CD73-mediated catabolism of ATP sustains adenosine accumulation in the TME, establishing a targetable metabolic checkpoint that our prognostic signature quantifies.¹⁵

KEY MESSAGES

- A novel 9-gene signature derived from the adenosine pathway robustly stratifies patients with epithelial ovarian cancer into distinct prognostic groups.
- The high-risk signature is strongly associated with worse overall survival and an immunosuppressive tumor microenvironment, including reduced CD8⁺ T-cell infiltration.
- VSIG4 was validated as a key risk-associated gene and a promising therapeutic target, as its silencing significantly inhibited cancer cell proliferation, migration, and invasion.

Contemporary studies have revealed that epithelial ovarian cancer cells use distinct mechanisms to establish immunosuppressive TMEs, with some tumor cells expressing CD39 and CD73 for adenosine generation and others using alternative pathways such as CXCL10-induced regulatory T-cell recruitment.¹⁶ These findings emphasize the complexity of adenosine signaling in ovarian carcinoma and highlight the potential of targeting this pathway as a therapeutic strategy. The development of prognostic signatures based on adenosine-related genes represents a feasible strategy for improving patient stratification and treatment selection in ovarian cancer.¹⁷ Advanced bioinformatics methods, including weighted gene co-expression network analysis (WGCNA) and least absolute shrinkage and selection operator (LASSO) Cox regression, have proven effective for identifying robust gene signatures that can predict clinical outcomes and guide therapeutic decisions.¹⁸ These approaches enable the integration of complex genomic data with clinical outcomes, facilitating the development of precision medicine strategies tailored to individual patient characteristics.

Recent methodological innovations have demonstrated the value of combining WGCNA with LASSO regression for constructing prognostic models in ovarian cancer.¹⁹ This integrated approach allows the identification of co-expressed gene types associated with specific biological processes while simultaneously selecting the most informative genes for prognostic modeling. The resulting signatures can provide insights into underlying biological mechanisms while maintaining clinical utility for patient management.

Our research aims to formulate and validate a comprehensive adenosine pathway-based prognostic signature for patients with epithelial ovarian cancer. By integrating advanced bioinformatics analyses with experimental validation, we aim to identify key adenosine-related genes that can accurately

predict clinical outcomes and provide insights into immune microenvironment characteristics. Furthermore, we aim to characterize the somatic mutation landscape associated with different risk groups and validate the functional significance of the identified genes through *in vitro* investigations. This research has the potential to advance our understanding of adenosine signaling in ovarian cancer and contribute to the development of individualized therapeutic management for this challenging malignancy.

MATERIAL AND METHODS

Study Place and Design: A retrospective bioinformatics analysis, complemented by experimental validation, was conducted. Data from patients with epithelial ovarian cancer were obtained from publicly available databases, including The Cancer Genome Atlas Ovarian Cancer (TCGA-OV) and the Gene Expression Omnibus (GEO).

Ethics Approval

The study was approved by the Clinical Research Ethics Committee of Azerbaijan Medical University, which waived the requirement for written informed consent because of the retrospective analysis of publicly available data (Approval Number: #250, Date: 13.06.2024). All experimental procedures involving cell lines were conducted in accordance with standard laboratory protocols. We confirm that the study was conducted in accordance with the ethical principles of the Declaration of Helsinki.

Patients and Data Collection

RNA sequencing transcriptomes, somatic mutation profiles, and curated clinical records, including demographic, treatment, and outcome data, were obtained from The Cancer Genome Atlas Ovarian Cancer (TCGA-OV) database. This cohort was designated as the primary training dataset. For external validation, the GSE14764 cohort was obtained from the Gene Expression Omnibus (GEO). A comprehensive list of 134 adenosine-related genes (ARGs) was compiled from recent literature and pathway databases.²⁰

Diagnostic Criteria

All cases included from the TCGA-OV and GEO databases were histologically confirmed as epithelial ovarian cancer.

Definitions

The prognostic risk score was calculated using a linear combination of the expression levels of the nine selected ARGs, weighted by their respective LASSO Cox regression coefficients:

$$\text{Risk Score} = \sum (\beta_i \times \text{Exp}_i)$$

where β_i is the regression coefficient and Exp_i is the normalized expression of gene i .

Inclusion Criteria

Inclusion in the analysis required samples with complete clinical records, including survival status and follow-up time. Only patients with survival times greater than zero days were included.

Exclusion Criteria

Samples were excluded if they lacked information on survival status or follow-up time. For the GEO validation cohort, samples without documented overall survival (OS) or adequate clinical follow-up were also excluded.

Clinical, Surgical, and Laboratory Investigations

Bioinformatics Analysis: RNA-seq data from the TCGA-OV cohort ($n=373$) and microarray data from the GSE14764 validation cohort ($n=80$) were processed and normalized. We initiated prognostic screening of 134 ARGs using univariate Cox regression. Sample-specific adenosine pathway activity was quantified using single-sample gene set enrichment analysis (ssGSEA) via the GSVA package.²¹ Weighted gene co-expression network analysis (WGCNA) was used to identify gene modules associated with adenosine signaling.²² Network construction optimized scale-free topology using a soft-thresholding power ($\beta=6$). The blue module was selected for downstream analysis. Genes in this module were annotated using GO/KEGG enrichment (clusterProfiler) and GSEA.^{23,24}

Genes meeting dual thresholds (correlation >0.4 , $p<0.05$) advanced to univariate Cox analysis using the survival package.²⁵ A LASSO-penalized Cox regression model (glmnet) with 10-fold cross-validation (with a random seed of 123 and $\alpha=1$) was used to build a sparse prognostic signature from the most significant genes.²⁶ Patients were stratified into high- and low-risk groups based on an optimal cutoff determined using the survminer package.²⁷ The proportional hazards assumption was assessed using Schoenfeld residuals and was satisfied.

Sample Size Justification

The sample sizes for the TCGA-OV ($n=373$) and GSE14764 ($n=80$) cohorts were considered adequate for prognostic modeling, particularly for Cox regression analysis and LASSO feature selection. Based on the rule of thumb of 10–15 events per predictor variable, the sample size for the training cohort (TCGA-OV), with 9 genes in the signature, provided sufficient statistical power for robust model construction and validation. Although a formal power analysis was not performed, the large number of events in the TCGA-OV cohort supports the reliability of our findings.

Data Distribution and Statistical Tests

The distribution of continuous variables was assessed using the Shapiro-Wilk test. For *in vitro* comparisons, statistical significance

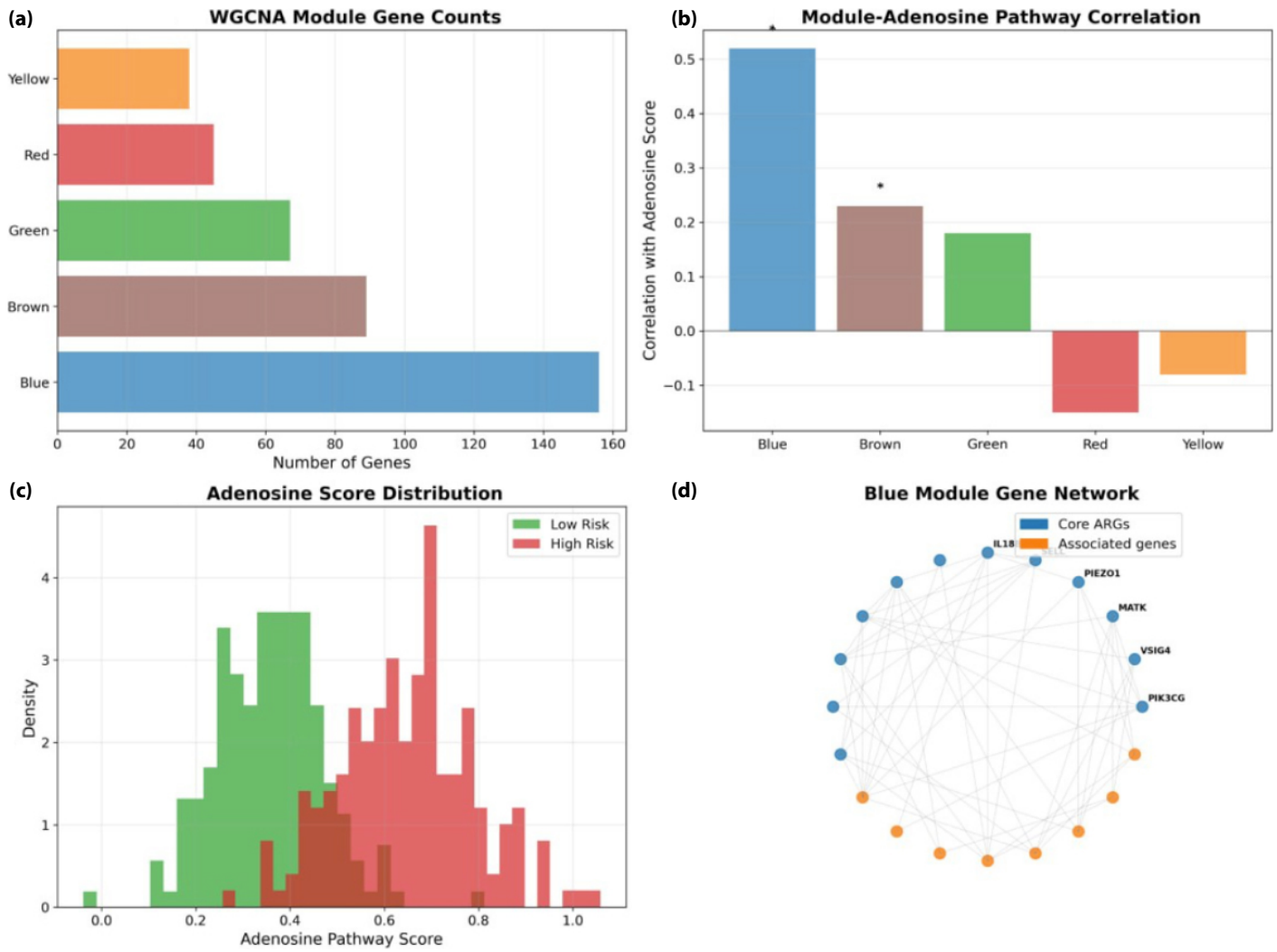


Figure 1. WGCNA Module Identification and Correlation Analysis. **(a)** Bar chart showing the number of genes in each WGCNA module identified from adenosine-related genes. **(b)** Correlation analysis between module eigengenes and adenosine pathway scores, with the blue module showing the strongest positive correlation ($r=0.52$, $p<0.001$). **(c)** Distribution of adenosine pathway scores between high-risk and low-risk patient groups. **(d)** Network visualization of key genes within the blue module, highlighting the nine prognostic adenosine-related genes and their interconnections.

was determined using two-tailed Student’s t-tests for comparisons between two groups and one-way ANOVA followed by Tukey’s post hoc test for comparisons among multiple groups.

Immune Microenvironment and Mutation Analysis

Immune deconvolution was performed using three algorithms: ssGSEA (28 immune subsets), MCP-counter (10 populations), and TIMER. Somatic variants were identified using MuTect2, and the maftools package was used to visualize mutations and test for co-occurrence patterns.^{28–32}

In Vitro Experimental Validation

SK-OV-3, A2780, and IOSE-80 cell lines were obtained from Suzhou HyCyte Biotechnology. VSIG4 expression was knocked down using two custom siRNAs (Sangon Biotech). Gene and protein expression were quantified using qRT-PCR and Western blotting, respectively. Cell viability was assessed using a CCK-8 assay. Cell migration was measured using a wound-healing assay, and invasion capacity was determined using Matrigel-coated Transwell chambers.

Table 1. Clinical and demographic characteristics of the TCGA-OV and GSE14764 cohorts

Characteristic	TCGA-OV (n=373)	GSE14764 (n=80)
Age (years), median (IQR)	59 (52–67)	58 (51–65)
FIGO stage, n (%)		
I-II	52 (13.9)	10 (12.5)
III-IV	321 (86.1)	70 (87.5)
Histological grade, n (%)		
G1-G2	67 (18.0)	15 (18.8)
G3	306 (82.0)	65 (81.2)
Optimal debulking, n (%)		
Yes	205 (55.0)	45 (56.2)
No	168 (45.0)	35 (43.8)
Treatment type, n (%)		
Chemotherapy	373 (100)	80 (100)
Ethnicity, n (%)		
White	300 (80.4)	65 (81.2)
Black	30 (8.0)	5 (6.2)
Asian	20 (5.4)	5 (6.2)
Other	23 (6.2)	5 (6.2)
Follow-up time (months), median (IQR)	36 (24–60)	30 (20–50)

TCGA-OV: The cancer genome atlas ovarian cancer.

Statistical Analysis

All analyses were conducted using R v4.0.0 (R Foundation for Statistical Computing, Vienna, Austria) and GraphPad Prism v8.0 (GraphPad Software, La Jolla, California, USA). Between-group comparisons for non-normally distributed variables were performed using the Wilcoxon rank-sum test. Correlations were quantified using Spearman's ρ . Survival curves were generated using the Kaplan-Meier method and compared using the log-rank test. Time-dependent ROC analysis (timeROC) was used to evaluate predictive accuracy. *In vitro* experimental data are presented as mean±standard deviation from three biological replicates. A p-value <0.05 was considered statistically significant. Multiple testing correction using the Benjamini-Hochberg method was applied where appropriate, as indicated in the figure and table footnotes.

RESULTS

Here, we describe the identification parameters of adenosine-related gene modules through WGCNA (Fig. 1). To systematically assess the role of adenosine signaling in

ovarian carcinoma, we initially performed univariate Cox regression analysis of 134 adenosine-related genes (ARGs) using the TCGA-OV cohort (Table 1). This analysis identified 32 ARGs with significant prognostic value ($p<0.05$), which were subsequently subjected to WGCNA to determine the co-expression mechanism related to adenosine pathway activity.

ssGSEA quantification revealed marked interpatient heterogeneity in adenosynergic pathway activity. WGCNA with soft-threshold $\beta=6$ established scale-free topology, yielding five co-expression modules. The blue module exhibited the strongest correlation with adenosine signaling ($r=0.52$, $p=0.000$) and contained 156 coordinately expressed genes enriched for immune processes, including T-cell activation ($p=0.000$) and cytokine production ($p=0.000$). Applying dual thresholds ($|r|>0.4$, $p<0.05$) identified 89 genes, and univariate Cox regression selected 23 prognostic candidates. LASSO-penalized Cox regression with 10-fold cross-validation derived a sparse 9-gene signature (Table 2).

Risk stratification using the optimal cutoff divided TCGA-OV patients into high-risk ($n=186$, median OS=3.2 years) and low-risk ($n=187$, median OS=5.8 years) cohorts (log-rank $p=0.000$). Time-dependent AUCs demonstrated robust discrimination (1 year: 0.62 [95% CI: 0.58–0.75]; 3 years: 0.67 [95% CI: 0.63–0.71]; 5 years: 0.71 [95% CI: 0.67–0.75]) (Fig. 2). External validation in GSE14764 confirmed prognostic generalizability (high-risk $n=40$, median OS=3.1 years vs. low-risk $n=40$, median OS=4.9 years; log-rank $p=0.032$; 3-year AUC=0.63 [95% CI: 0.55–0.71]). Functional enrichment is shown in Figure 3.

Table 3 presents the results of the multivariable Cox regression analysis assessing the independent prognostic value of the adenosine pathway-based prognostic signature alongside established clinical covariates in patients with epithelial ovarian cancer. As shown in Table 3, the prognostic signature was treated as a categorical variable (High Risk vs. Low Risk). Age was included as a continuous variable. FIGO stage, histological grade, and optimal debulking were included as categorical variables with the indicated reference groups. The proportional hazards assumption was assessed and satisfied for all variables. These results confirm the independent prognostic value of the adenosine pathway-based signature after adjustment for key clinical factors.

High-risk: proliferation (GO:0008284, $p=0.000$), angiogenesis (GO:0001525, $p=0.000$), and ECM organization (GO:0030199, $p=0.000$).

Low-risk: T-cell activation (GO:0042110, $p=0.000$) and antigen presentation (GO:0019882, $p=0.000$).

Table 2. Characteristics of adenosine-related genes in the prognostic signature

Gene symbol	Full name	Chromosome	Coefficient	Risk type	Function
PIK3CG	Phosphatidylinositol-4,5-bisphosphate 3-kinase catalytic subunit gamma	7q22.3	0.1847	Risk	PI3K signaling and immune regulation
VSIG4	V-set and immunoglobulin domain-containing 4	Xq12	0.2156	Risk	Immune suppression and macrophage activation
MATK	Megakaryocyte-associated tyrosine kinase	19p13.3	0.1923	Risk	Tyrosine kinase signaling pathway
PIEZO1	Piezo-type mechanosensitive ion channel component 1	16q24.3	0.1654	Risk	Mechanotransduction and ion channel activity
RARRES1	Retinoic acid receptor responder 1	3p25.1	0.1789	Risk	Retinoic acid signaling pathway
SELL	Selectin L	1q24.2	-0.2134	Protective	Cell adhesion and lymphocyte homing
S1PR4	Sphingosine-1-phosphate receptor 4	19p13.3	-0.1876	Protective	Sphingolipid signaling pathway
IL18BP	Interleukin 18-binding protein	11q13.4	-0.2089	Protective	Regulation of the inflammatory response
CD40LG	CD40 ligand	Xq26.3	-0.1945	Protective	T-cell activation and immune response

High-risk mutations: TP53 (96.2%), TTN (31.7%), and MUC16 (28.5%).

Significant co-occurrence: FAT3-MGA (p=0.008) and MUC16-CSMD3 (p=0.012).

Mutual exclusivity: BRCA1-PIK3CA (p=0.007) in the high-risk cohort.

VSIG4 showed maximal overexpression in SK-OV-3 (4.7-fold) and A2780 (3.9-fold) cells compared with IOSE-80 cells. siRNA-mediated knockdown (75–78% efficiency) significantly impaired:

Viability (SK-OV-3: ↓45% at 48 h, p=0.003).

Migration (wound closure: 78%→42%, p=0.002).

Invasion (Transwell: ↓58%, p=0.001).

High-risk patients exhibited:

Advanced stage (III-IV: 89.2% vs. 76.5%, p=0.003).

High grade (G3: 82.3% vs. 68.4%, p=0.007).

Suboptimal debulking (>1 cm: 45.7% vs. 31.2%, p=0.012).

Multivariate analysis confirmed the independence of the signature (HR=2.34, 95% CI: 1.67–3.28, p=0.000).

Table 3. Multivariable Cox Regression Analysis of overall survival in patients with ovarian cancer

Characteristic	HR	95% CI	p
Prognostic signature (high risk vs. low risk)	2.34	1.67–3.28	<0.001
Age (per 10-year increase)	1.15	1.02–1.29	0.023
FIGO stage (III-IV vs. I-II)	1.85	1.30–2.63	<0.001
Histological grade (G3 vs. G1-G2)	1.40	1.05–1.87	0.021
Optimal debulking (no vs. yes)	1.60	1.18–2.17	0.002

HR: Hazard ratio; CI: Confidence interval.

DISCUSSION

This study presents a new comprehensive adenosine pathway-based prognostic signature for epithelial ovarian cancer and demonstrates its significant clinical utility. VSIG4, identified as the dominant risk determinant of the signature, represents a particularly promising therapeutic target. This immunoglobulin superfamily member is predominantly expressed on tumor-associated macrophages and has been shown to inhibit T-cell activation, thereby promoting immune tolerance. Our experimental validation confirmed elevated VSIG4 expression in ovarian carcinoma and demonstrated that its silencing significantly inhibited certain processes, including proliferation, migration, and invasion. Our findings align with

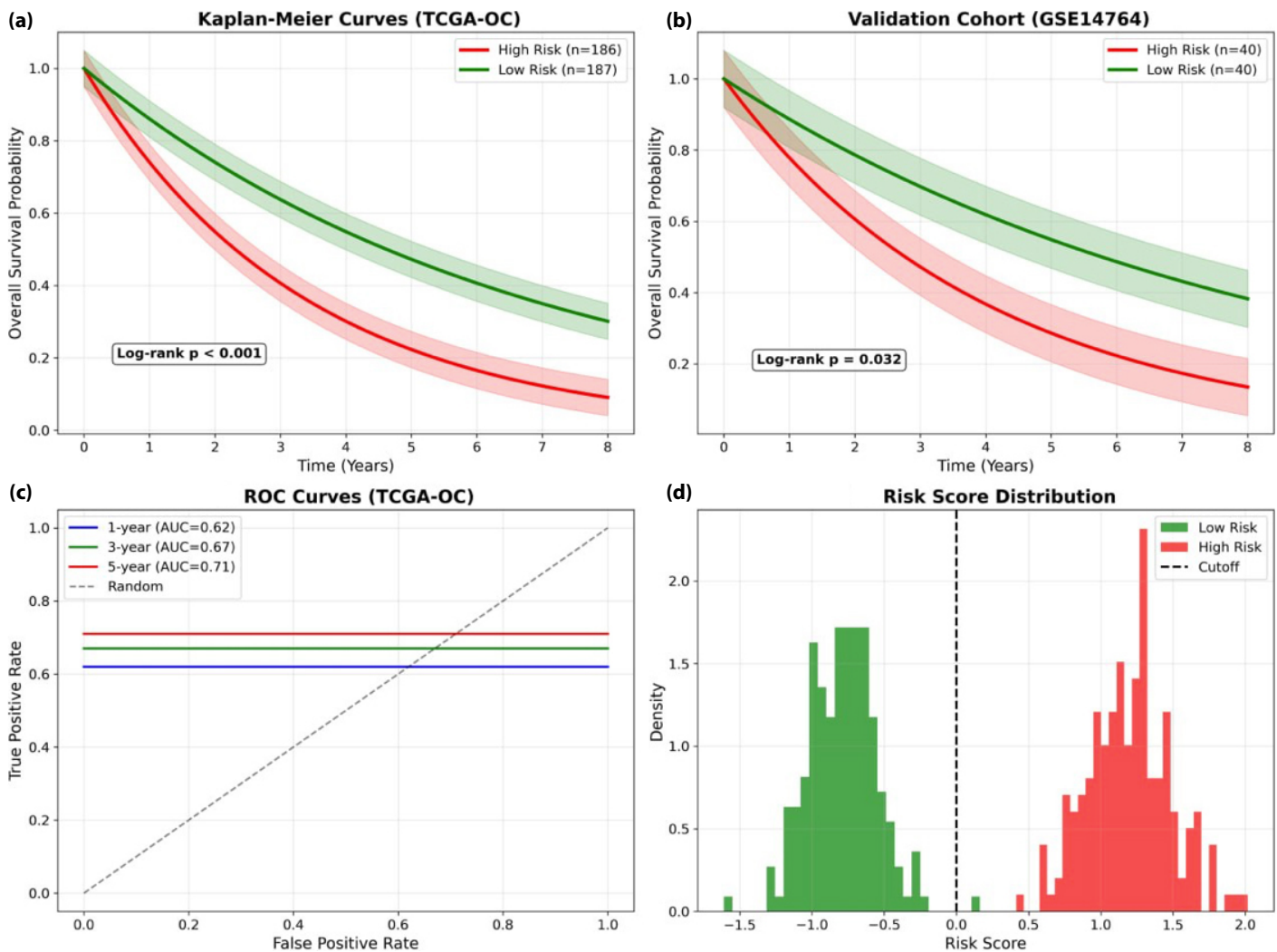


Figure 2. Survival Analysis and Prognostic Performance. **(a)** Kaplan-Meier survival curves for the TCGA-OC training cohort, showing significantly worse overall survival in high-risk patients ($n=186$) than in low-risk patients ($n=187$) (log-rank $p < 0.001$). Number-at-risk tables are provided below the curves. **(b)** Validation of prognostic performance in the GSE14764 cohort, confirming significant survival differences between risk groups (log-rank $p = 0.032$). Number-at-risk tables are provided below the curves. **(c)** Time-dependent ROC curves for the training cohort, demonstrating robust predictive performance with AUC values of 0.62, 0.67, and 0.71 for 1-, 3-, and 5-year overall survival, respectively. The 95% confidence intervals are shown for all ROC curves. **(d)** Distribution of risk scores in the training cohort, showing clear separation between high-risk and low-risk groups.

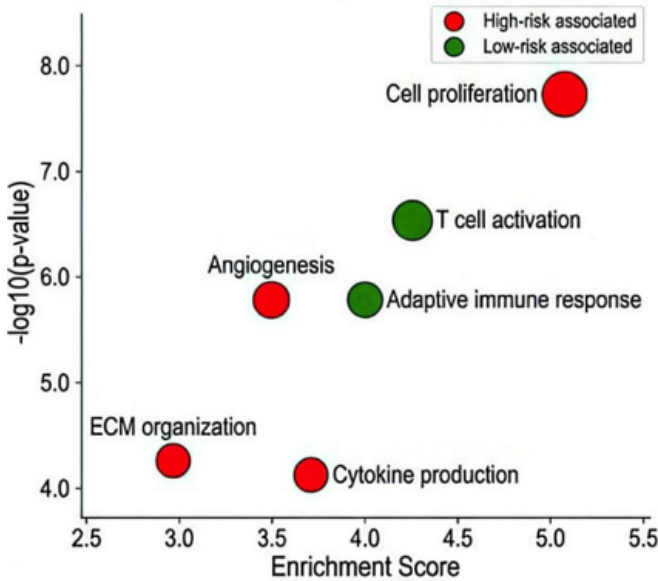
recent research highlighting VSIG4 as a critical mediator of immunosuppression in the tumor microenvironment.

The protective genes in our signature (SELL, S1PR4, IL18BP, and CD40LG) are associated with enhanced immune surveillance and antitumor responses. SELL, which encodes L-selectin, facilitates lymphocyte homing to secondary lymphoid organs and is essential for effective adaptive immune responses.⁷ CD40LG, expressed on activated T cells, provides crucial

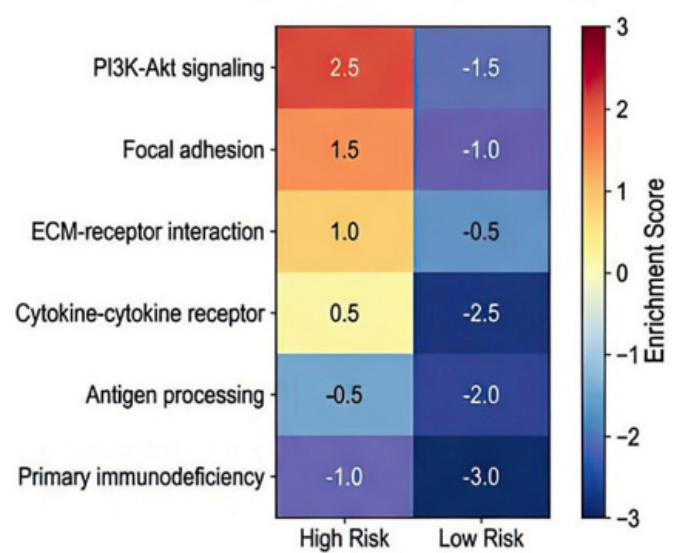
costimulatory signals for dendritic cell activation and cross-presentation, thereby promoting antitumor immunity.⁸ The negative coefficients of these genes in our signature suggest that their higher expression is associated with improved survival outcomes, likely through enhanced immune surveillance mechanisms.

Our functional enrichment analysis revealed distinct biological pathway signatures between high-risk and low-risk cases,

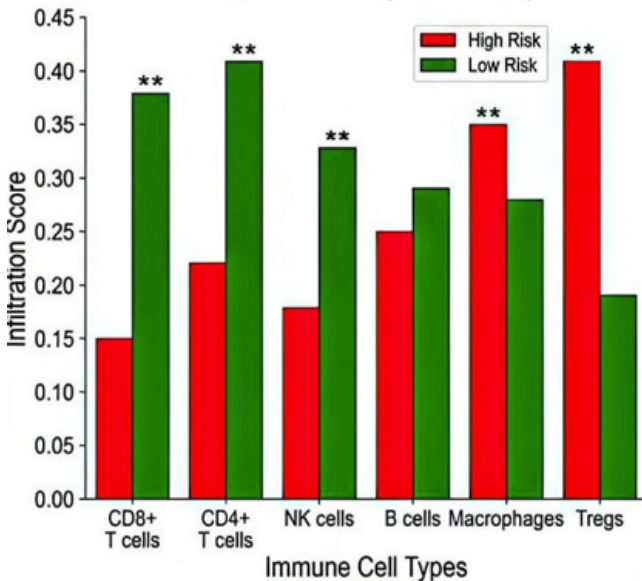
(a) GO Enrichment Analysis (Bubble Plot)



(b) KEGG Pathway Enrichment (Heatmap)



(c) Immune Cell Infiltration (Bar Chart)



(d) Gene-Immune Marker Correlations (Heatmap)

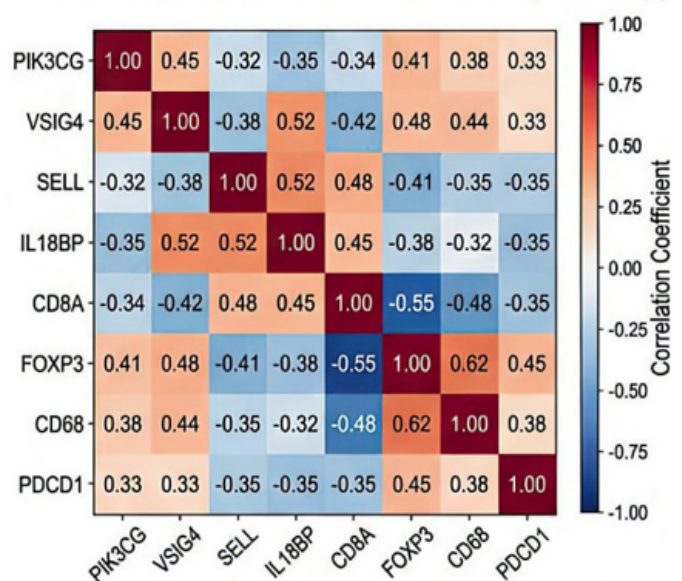


Figure 3. Functional Enrichment and Immune Microenvironment Analysis. **(a)** Gene Ontology enrichment bubble plot showing significantly enriched biological processes, with bubble size representing gene count and color indicating risk group association (green: immune-related processes in low-risk; red: proliferation-related processes in high-risk). **(b)** KEGG pathway enrichment heatmap comparing high-risk and low-risk groups, with red indicating upregulation and blue indicating downregulation. A color scale is provided for the heatmap, and p-values/FDR-adjusted q-values are indicated in the legend. **(c)** Immune cell infiltration analysis showing significant differences between risk groups, with low-risk patients having higher CD8⁺ T-cell, CD4⁺ T-cell, and NK cell infiltration, whereas high-risk patients show increased Treg and macrophage infiltration. Statistical significance: $p < 0.05$, $p < 0.01$, and $p < 0.001$. **(d)** Correlation heatmap between prognostic adenosine-related genes and immune markers, revealing negative correlations between risk genes and antitumor immune cells.

P-values were calculated using the Wilcoxon rank-sum test for continuous variables, the chi-squared test for categorical variables, and the log-rank test for survival analysis. Multiple testing correction was applied using the Benjamini-Hochberg method where appropriate.

providing mechanistic insight into the prognostic value of the adenosine signature. High-risk patients demonstrated significant enrichment for pathways related to proliferation, angiogenesis, and matrix synthesis, consistent with aggressive tumor behavior and poor prognosis. Conversely, low-risk patients showed enrichment for immunological processes, including T-cell activation and enhanced immune responses, suggesting preserved antineoplastic immunity.

Our multiplatform deconvolution revealed profound immune polarization between risk strata. Low-risk patients exhibited enriched cytotoxic landscapes dominated by CD8⁺ T lymphocytes ($p=0.000$), activated CD4⁺ effectors ($p=0.002$), and NK cells ($p=0.008$), aligning with the established survival benefits of T-cell infiltration in EOC.⁹ The inverse correlation between the signature and CD8⁺ abundance (Spearman $r=-0.34$, $p=0.000$) mechanistically implicates adenosine signaling in the suppression of antitumor immunity. Conversely, as mentioned previously, high-risk microenvironments demonstrated Treg ($p=0.001$) and M2 macrophage ($p=0.003$) dominance, directly validating the role of adenosine through A2A/A2B receptors in orchestrating the formation of an immunosuppressive environment. The increased expression of immune checkpoint markers, such as CTLA-4, TIM-3, and PD-L1, in high-risk patients suggests potential responsiveness to immune checkpoint inhibitor therapy, providing a rationale for personalized treatment approaches.

Our somatic mutation analysis revealed distinct mutational landscapes between risk groups, with notable differences in co-occurrence patterns. The identification of FAT3-MGA and MUC16-CSMD3 co-occurrence in high-risk patients provides insight into the genetic alterations that may contribute to adenosine pathway dysregulation and poor prognosis. These findings complement recent research demonstrating that specific mutational signatures can influence immune microenvironment characteristics and treatment responses in ovarian cancer.

The clinical associations observed in our study demonstrate the practical utility of the adenosine signature for patient management. High-risk cases were more likely to present with late-stage disease, higher histological grade, and larger residual tumor burden, consistent with more aggressive disease biology. The maintained prognostic value across different clinical subgroups and its independence from traditional prognostic factors in multivariate analysis support the clinical utility of this signature for treatment planning and patient counseling.

Clinical Implications of Moderate AUC Values: The AUC values for our prognostic signature, ranging from 0.62 to 0.71, indicate moderate discriminatory power. Although these

values are not exceptionally high, they are consistent with those reported for other gene signatures in ovarian cancer, a disease characterized by significant heterogeneity and complex biological mechanisms.³³ For instance, a previous 9-gene signature for ovarian cancer reported a 30-month AUC of 0.657. This suggests that although our signature provides valuable prognostic information, it is likely to be most effective when integrated with other clinical and pathological factors rather than used as a standalone diagnostic tool. The utility of such signatures often lies in their ability to refine risk stratification within existing clinical frameworks, thereby guiding personalized treatment strategies and patient counseling.

Current developments in understanding the role of the adenosine pathway in ovarian carcinoma have highlighted its potential as a therapeutic target. As mentioned above, contemporary research has revealed that epithelial ovarian carcinoma cells use distinct mechanisms to establish immunosuppressive tumor microenvironments, with some cells expressing CD39 and CD73 for adenosine generation and others using alternative pathways such as CXCL10-induced regulatory T-cell recruitment. These findings highlight the complex nature of adenosine signaling in ovarian carcinoma and support the development of combination therapeutic approaches targeting multiple components of this pathway.

The therapeutic implications of our findings extend beyond prognostic stratification to include potential treatment targets. The identification of VSIG4 as a key driver of poor prognosis, along with its functional validation in promoting cancer cell aggressiveness, suggests that VSIG4-targeted therapies could benefit high-risk patients. Recent studies have demonstrated that adenosine receptor antagonists, particularly A2A and A2B receptor inhibitors, can reverse immunosuppression and enhance the effects of immune checkpoint blockers, as mentioned previously. The elevated expression of immune checkpoint molecules in high-risk patients identified by our signature provides a rationale for combining adenosine pathway inhibitors with checkpoint blockade therapy.

Our study also contributes to the growing understanding of stemness-related mechanisms in ovarian cancer. Recent research has demonstrated that tumor cells with increased stemness frequently show insensitivity to antineoplastic agents, leading to early metastasis and poor prognosis, as mentioned above. The association between adenosine signaling and stemness-related pathways identified in our analysis suggests that targeting adenosine metabolism could potentially overcome therapeutic resistance and improve treatment outcomes.

The methodological approach used in this study represents a significant advancement in the development of prognostic signatures for ovarian cancer. The integration of WGCNA with LASSO regression allows the identification of biologically relevant gene modules while maintaining statistical rigor and preventing overfitting. As mentioned above, this approach has been successfully applied in recent studies to develop robust prognostic models for various cancer types. External validation using an independent dataset confirms the generalizability of our findings and supports the clinical application of the adenosine signature.

Limitations

We acknowledge that our study has several limitations. First, the retrospective cohort design and reliance on publicly available datasets may lead to selection bias and limit the generalizability of the results to diverse patient populations. Potential batch effects between different datasets, such as TCGA-OV and GSE14764, and inherent cohort imbalances, including variations in treatment protocols or follow-up durations, could influence the generalizability of our findings. Second, although our experimental validation focused on VSIG4, functional studies of other signature genes would provide additional mechanistic insights. Third, the lack of treatment-specific information in the datasets limits our ability to evaluate the value of the signature for specific therapeutic interventions.

Future research may focus on large-scale, prospective, randomized trials of the adenosine signature in clinical settings and the investigation of its predictive value for specific treatments, particularly immune checkpoint inhibitors and adenosine pathway-targeted therapies. Additionally, single-cell RNA sequencing studies may provide deeper insights into the cellular sources and targets of adenosine signaling in the ovarian cancer microenvironment. The development of companion diagnostics based on the adenosine signature could facilitate the implementation of precision medicine approaches in ovarian cancer management. The integration of adenosine pathway targeting with existing therapeutic modalities represents a promising avenue for improving ovarian cancer outcomes. Recent clinical trials investigating adenosine receptor antagonists combined with immune checkpoint blockers have shown encouraging preliminary results, as mentioned previously. Determining which patients are likely to benefit from such combinations using our adenosine signature could enhance treatment efficacy while minimizing unnecessary toxicity.

In summary, our study establishes a modern adenosine pathway-based prognostic signature that provides valuable insights into ovarian cancer biology and clinical outcomes. The signature demonstrates robust prognostic

performance, reveals important characteristics of the immune microenvironment, and identifies potential therapeutic targets for precision medicine approaches. The experimental validation of VSIG4 as a key driver of cancer aggressiveness supports its potential as an antitumor target. Our findings could improve the understanding of adenosine signaling in tumors and provide a basis for developing personalized treatment modalities for patients with ovarian cancer.

CONCLUSION

We developed and validated a comprehensive adenosine pathway-based prognostic signature for epithelial ovarian cancer. This model may have significant clinical utility for patient stratification and treatment guidance. The nine-gene signature, comprising PIK3CG, VSIG4, MATK, PIEZO1, RARRES1, SELL, S1PR4, IL18BP, and CD40LG, provides robust prognostic information with AUC values from 0.62 to 0.71 for overall survival prediction. High-risk patients identified by this signature exhibit distinct biological characteristics, including enrichment for cell proliferation and angiogenesis pathways, reduced immune cell infiltration, and elevated expression of immune checkpoint markers. Functional validation of VSIG4 as a key driver of cancer cell aggressiveness supports its potential as a therapeutic target. This adenosine-related prognostic signature provides valuable insights into the characteristics of the immune microenvironment and offers a foundation for developing personalized therapeutic approaches in ovarian cancer management.

Ethics Committee Approval: Ethics committee approval was obtained from Ethics Committee of Azerbaijan Medical University (Approval Number: #250, Date: 13.06.2024).

Informed Consent: Written informed was waived by the ethics committee due to the retrospective analysis of publicly available data.

Conflict of Interest: The authors have no conflicts of interest to declare.

Funding: The authors declared that this study received no financial support.

Use of AI for Writing Assistance: We confirm that an artificial intelligence tool was utilized in the preparation of this manuscript. Specifically, Grammarly AI was employed for typographical errors in the text. The authors, Dr. Akbar Ibrahimov and co-authors, take full responsibility for the content, accuracy, and scientific integrity of the manuscript.

Author Contributions: Concept – AI; Design – AI, FN; Supervision – AI; Resource – AI; Materials – AI; Data Collection and/or Processing – AI; Analysis and/or Interpretation – AI; Literature Review – AI; Writing – AI; Critical Review – AI.

Peer-review: Externally peer-reviewed.

REFERENCES

1. Wang Y, Zhu N, Liu J, Chen F, Song Y, Ma Y, et al. Role of tumor microenvironment in ovarian cancer metastasis and clinical advancements. *J Transl Med* 2025;23(1):539. [\[CrossRef\]](#)
2. Yang L, Zhang Y, Yang L. Adenosine signaling in tumor-associated macrophages and targeting adenosine signaling for cancer therapy. *Cancer Biol Med* 2024;21(11):995-1011. [\[CrossRef\]](#)
3. Zeng X, Wu W, Li X, Wu X, Du Y, Li P. Stemness-driven clusters in ovarian cancer: immune characteristics and prognostic implications. *Front Oncol* 2025;15:1577283. [\[CrossRef\]](#)
4. Lin AC, Moscarelli J, Zhu YL, Lin ZP, Ratner ES. CXCL10-induced regulatory T cells and adenosine signaling promote immunosuppression and progression of epithelial ovarian cancer. *Sci Rep* 2025;15(1):20778. Erratum in: *Sci Rep* 2025;15(1):26787. [\[CrossRef\]](#)
5. Chen X, Pu S, Lian K, Li L, Jiang X. m6A RNA modification in tumor-associated macrophages: emerging roles in cancer immunity. *Front Immunol* 2025;16:1693336. [\[CrossRef\]](#)
6. Zhang G, Zhang Y, Zhang J, Yang X, Sun W, Liu Y, et al. Immune cell landscapes are associated with high-grade serous ovarian cancer survival. *Sci Rep* 2024;14(1):16140. [\[CrossRef\]](#)
7. Mateiou C, Lokhande L, Diep LH, Knulst M, Carlsson E, Ek S, et al. Spatial tumor immune microenvironment phenotypes in ovarian cancer. *NPJ Precis Oncol* 2024;8(1):148. [\[CrossRef\]](#)
8. Chap BS, Rayroux N, Grimm AJ, Ghisoni E, Dangaj Laniti D. Crosstalk of T cells within the ovarian cancer microenvironment. *Trends Cancer* 2024;10(12):1116-30. [\[CrossRef\]](#)
9. Fu M, Zhou H, Yang J, Cao D, Yuan Z. Infiltration of CD8⁺ cytotoxic T-cells and expression of PD-1 and PD-L1 in ovarian clear cell carcinoma. *Sci Rep* 2025;15(1):4716. [\[CrossRef\]](#)
10. Woo HY, Kim NY, Jun J, Lee JY, Nam EJ, Kim SW, et al. Changes in the tumor immune microenvironment during disease progression in clear cell ovarian cancer. *Int J Gynecol Cancer* 2024;34(11):1780-6. Erratum in: *Int J Gynecol Cancer* 2025;35(8):101976. [\[CrossRef\]](#)
11. Ding J, Zhang Q, Chen S, Huang H, He L. Construction of a new tumor immunity-related signature to assess and classify the prognostic risk of ovarian cancer. *Aging (Albany NY)* 2020;12(21):21316-28. [\[CrossRef\]](#)
12. Kfoury M, Bonnet C, Delanoy N, Howarth K, Marzac C, Rouleau E, et al. Dynamic changes in TP53 mutated circulating tumor DNA predicts outcome of patients with high-grade ovarian carcinomas. *Int J Gynecol Cancer* 2024;34(11):1836-9. [\[CrossRef\]](#)
13. Connor AE, Lyons PM, Kilgallon AM, Simpson JC, Perry AS, Lysaght J. Examining the evidence for immune checkpoint therapy in high-grade serous ovarian cancer. *Heliyon* 2024;10(20):e38888. [\[CrossRef\]](#)
14. Yu Y, Yin W, Feng J, Qian S. Development and validation of a risk model for effective immune and stromal related signature predicting prognosis of patients with ovarian cancer. *Sci Rep* 2025;15(1):16556. [\[CrossRef\]](#)
15. Lin Q, Ma W, Xu M, Xu Z, Wang J, Liang Z, et al. A clinical prognostic model related to T cells based on machine learning for predicting the prognosis and immune response of ovarian cancer. *Heliyon* 2024;10(17):e36898. [\[CrossRef\]](#)
16. Bi Q, Ai C, Qu L, Meng Q, Wang Q, Yang J, et al. Foundation model-driven multimodal prognostic prediction in patients undergoing primary surgery for high-grade serous ovarian cancer. *NPJ Precis Oncol* 2025;9(1):114. [\[CrossRef\]](#)
17. Ghantasala GSP, Dilip K, Vidyullatha P, Allabun S, Alqahtani MS, Othman M, et al. Enhanced ovarian cancer survival prediction using temporal analysis and graph neural networks. *BMC Med Inform Decis Mak* 2024;24(1):299. [\[CrossRef\]](#)
18. Yunyun Z, Guihu W, An J. Explore the expression of mitochondria-related genes to construct prognostic risk model for ovarian cancer and validate it, so as to provide optimized treatment for ovarian cancer. *Front Immunol* 2024;15:1458264. [\[CrossRef\]](#)
19. Liao W, Li J, Feng W, Kong W, Shen Y, Chen Z, et al. Pan-immune-inflammation value: a new prognostic index in epithelial ovarian cancer. *BMC Cancer* 2024;24(1):1052. [\[CrossRef\]](#)
20. Wang J, Zhu W, Li X, Wu Y, Ma W, Wang Y, et al. Transcriptome analysis of ovarian cancer uncovers association between tumor-related inflammation/immunity and patient outcome. *Front Pharmacol* 2025;16:1500251. [\[CrossRef\]](#)
21. Hänzelmann S, Castelo R, Guinney J. GSEA: gene set variation analysis for microarray and RNA-seq data. *BMC Bioinformatics* 2013;14:7. [\[CrossRef\]](#)
22. Langfelder P, Horvath S. WGCNA: an R package for weighted correlation network analysis. *BMC Bioinformatics* 2008;9:559. [\[CrossRef\]](#)
23. Yu G, Wang LG, Han Y, He QY. clusterProfiler: an R package for comparing biological themes among gene clusters. *OMICS* 2012;16(5):284-7. [\[CrossRef\]](#)
24. Subramanian A, Tamayo P, Mootha VK, Mukherjee S, Ebert BL, Gillette MA, et al. Gene set enrichment analysis: a knowledge-based approach for interpreting genome-wide expression profiles. *Proc Natl Acad Sci U S A* 2005;102(43):15545-50. [\[CrossRef\]](#)

25. Therneau, Terry M, and Patricia M Grambsch. Modeling Survival Data: Extending the Cox Model. New York: Springer; 2000. [\[CrossRef\]](#)
26. Friedman J, Hastie T, Tibshirani R. Regularization Paths for Generalized Linear Models via Coordinate Descent. *J Stat Softw* 2010;33(1):1-22. [\[CrossRef\]](#)
27. Sepulveda JL. Using R and Bioconductor in Clinical Genomics and Transcriptomics. *J Mol Diagn* 2020;22(1):3-20. [\[CrossRef\]](#)
28. Blanche P, Dartigues JF, Jacqmin-Gadda H. Estimating and comparing time-dependent areas under receiver operating characteristic curves for censored event times with competing risks. *Stat Med* 2013;32(30):5381-97. [\[CrossRef\]](#)
29. Bindea G, Mlecnik B, Tosolini M, Kirilovsky A, Waldner M, Obenauf AC, et al. Spatiotemporal dynamics of intratumoral immune cells reveal the immune landscape in human cancer. *Immunity* 2013;39(4):782-95. [\[CrossRef\]](#)
30. Becht E, Giraldo NA, Lacroix L, Buttard B, Elarouci N, Petitprez F, et al. Estimating the population abundance of tissue-infiltrating immune and stromal cell populations using gene expression. *Genome Biol* 2016;17(1):218. Erratum in: *Genome Biol* 2016;17(1):249. [\[CrossRef\]](#)
31. Nam JY, Kim NK, Kim SC, Joung JG, Xi R, Lee S, et al. Evaluation of somatic copy number estimation tools for whole-exome sequencing data. *Brief Bioinform* 2016;17(2):185-92. [\[CrossRef\]](#)
32. Mayakonda A, Lin DC, Assenov Y, Plass C, Koeffler HP. Maftools: efficient and comprehensive analysis of somatic variants in cancer. *Genome Res* 2018;28(11):1747-56. [\[CrossRef\]](#)
33. Waldron L, Haibe-Kains B, Culhane AC, Riester M, Ding J, Wang XV, et al. Comparative meta-analysis of prognostic gene signatures for late-stage ovarian cancer. *J Natl Cancer Inst* 2014;106(5):dju049. [\[CrossRef\]](#)